JOURNAL OF ENGINEERING annals OF FACULTY OF ENGINEERING HUNEDOARA

MICROSTRUCTURE EVOLUTION OF CrMoV WELD METAL AFTER LONG-TERM HEAT EXPOSURE IN THE SUB-CREEP RANGE

Petr MOHYLA [1], Ivo HLAVATÝ [1], Eva SCHMIDOVÁ[2]

[1]VŠB - Technical University of Ostrava, Faculty of Engineering,
Dept. of Mechanical Technology, CZECH REPUBLIC
[2] University of Pardubice, Jan Perner Transport Faculty, CZECH REPUBLIC

ABSTRACT
The mechanical properties of 0,5%Cr-0,5%Mo-0,3%V steels are affected in particular by the parameters of the dispersion phase, namely vanadium carbides and carbonitrides MX. The dispersion of MX particles occurs during steel tempering, but subsequent long-term heat exposure causes changes in the number, mean size and mean spacing of particles. These changes significantly influence the material's mechanical properties. This article presents the results of a microstructural analysis which quantifies changes in the dispersion phase in 0,5%Cr-0,5%Mo-0,3%V weld metal during exposure in the sub-creep range.
Key words:
CrMoV steel welds, the sub-creep range, secondary hardening, vanadium carbides and carbonitrides, microstructural analysis, image analysis

1. INTRODUCTION

Low-alloy creep-resistant steels type 0,5%Cr-0,5%Mo-0,3%V are extensively used in power and chemical industry for fabrication of tubes, pipes and forgings. Their long-term creep resistance, expressed as creep strength after 10^5 hours, is significantly higher in comparison to CrMo steels. The other significant property of high creep-resistant steels containing vanadium is their demanding technological processing, which stems from the dominant affect of the dispersion phase on their mechanical properties. Dispersion phase parameters especially affect heat treatment. Vanadium carbides and carbonitrides (MX), which play a key role in CrMoV steels, precipitate particularly during tempering.

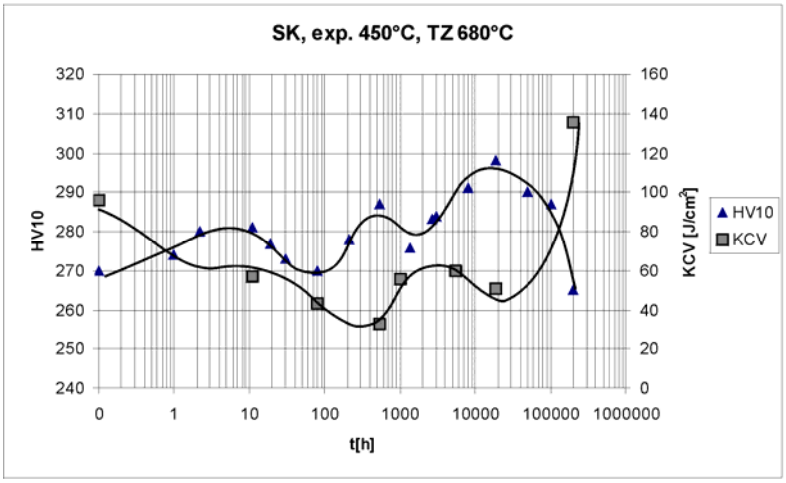

Fig. 1 Hardness (HV) and impact toughness (KCV) of CrMoV weld metal at operating temperature 450°C, tempered at 680°C/2h

However, during long-term heat exposure the number, mean size and mean spacing of particles changes. These changes significant influence mechanical properties and thereby even the durability and operating reliability of power equipment. Operation in the sub-creep region, which in the case of the tested steel 14MoV6-3 has a top limit temperature of approx. 480

°C, causes secondary hardening, accompanied by a decrease in impact toughness. The mentioned secondary hardening is especially pronounced in weld joints which were tempered at temperatures lower than is required by the material specification, i.e. temperatures lower than 720°C. Fig. 1 shows the changes in hardness and impact toughness of weld metal tempered at 680°C.

2. METHODOLOGY

Experimental parent material was a pipe grade 15128 (14MoV6-3), D324x32mm. Weld joints were produced by MMAW (111) with an electrode EB321 – E Z(CRMoV) B 22 according EN 1599. Chemical composition of pipe and consumables is given in table 1. A microanalysis was performed to confirm additional precipitation of MX particles and changes in weld joint mechanical properties.

As input material for microstructural analysis served weld metal samples tempered to 680°C, and after subsequent heat exposure.

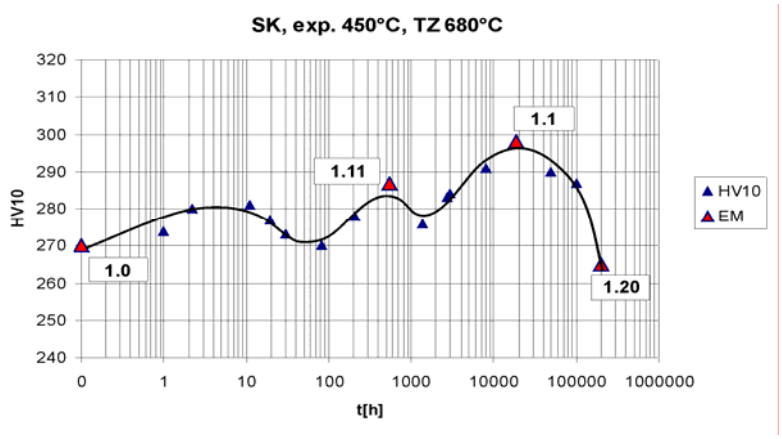

Fig. 2 Selected samples for electron microstructural analysis

- sample 1.0: initial condition
- sample 1.11: after annealing 500°C/23,4 h
- sample 1.1: after annealing 550°C/50,4 h
- sample 1.20: after annealing 550°C/546,5 h

These samples are highlighted in Fig. 2, where times of exposure are recalculated for equivalent temperature of 450°C using Arrhenius formula with Activation energy Q=292 kJ/mol [6,7,8].

Table 1: Chemical composition of experimental materials in mass %

	C	Mn	Si	Cr	Mo	V	Ti	Al	N
14MoV6-3	0,16	0,61	0,29	0,52	0,37	0,24	0,0195	0,019	0,005
weld metal	0,15	0,67	0,30	0,58	0,42	0,26	0,010	0,022	0,052

The electron-microscope study was conducted using transmission electron microscope, equipped with an energy dispersion analyser. Identification of minority phases was performed using a combination of electron diffraction and qualitative energy dispersion analysis of particles present on extraction carbon replicas. This metal foils were prepared by jet polishing in an electrolyte at room temperature and under voltage U = 80 V.

3. RESULTS

The weld metal microstructure contains a mixture of ferrite and bainite. Results of minority phase study in the samples are presented in Table 2. It is evident that all samples contained particles of cementite and MX particles, where M = V, X = C, N. A typical example of precipitate distribution in extraction carbon plates is presented in Fig. 3. Fine MX particles precipitated inside ferrite and bainitic ferrite grains, while the relatively coarse cementite grains usually lined the bainitic ferrite boundary. The fibrous morphology of MX particles was not seen in studied samples. Furthermore, weld metal included numerous globular particles of complex silicon, manganese and titanium oxides.

Table 2. Minority phase identification results

sample	minority phase
1.0	MX, M_3C
1.11	MX, M_3C
1.1	MX, M_3C
1.20	MX, M_3C

Dislocation density was determined in bainitic ferrite plates. Dislocation density was calculated using the Hamo method:

$$\rho = \left(\left(\frac{N_1}{L_1}\right) + \left(\frac{N_2}{L_2}\right)\right) \cdot \frac{1}{t} \cdot X \ [m^{-2}] \qquad (1)$$

where: N1 , N2, number of intersections of two parallel lines with dislocations
L1 , L2, total length of lines
t , foil thickness, we selected t = 125 nm
X, factor considering the share of non-visible dislocations for the selected imaging diffraction conditions.

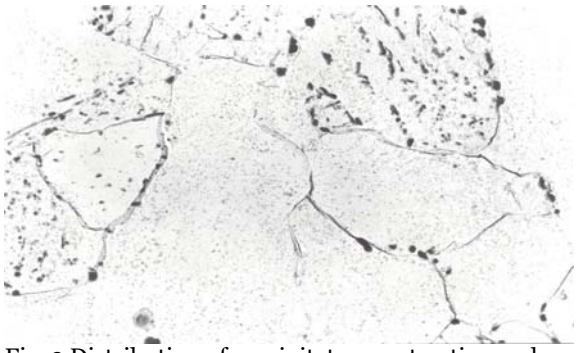

Fig. 3 Distribution of precipitate on extraction carbon replica, sample 1.0, magnification: 9000x

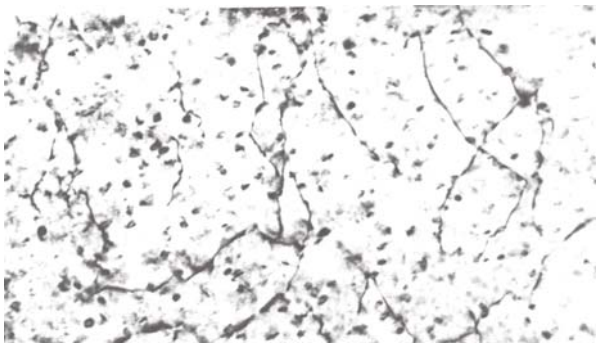

Fig. 4 Dislocation substructure of weld metal, thin foil, sample 1.20, magnification: 109 000x

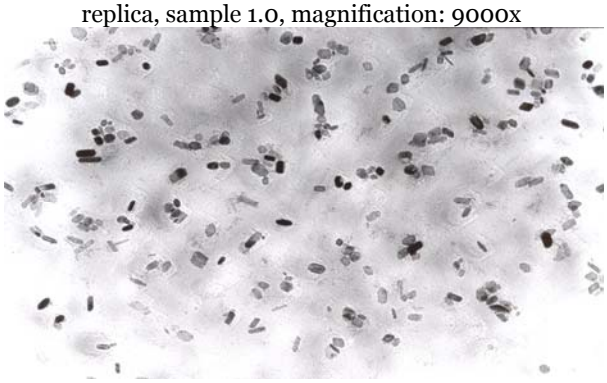

Fig. 5 Dispersion of MX particles, weld metal – bainite, extraction carbon replica, sample 1.20, magnification: 151 000x

Table 3 The density of dislocations

sample	$\rho.10^{-14}$ [m^{-2}]
1.0	4,91 ± 0,94
1.11	4.26 ± 0,97
1.1	4,50 ± 0,66
1.20	3,60 ± 0,95

The density of dislocations in individual samples was assessed on photographs with a total magnification of 109 000x, see Fig. 4. Measurement results (arithmetic mean and standard deviation) are presented in Table 3. The number of particles per unit area (n_s) was calculated as a proportion of the number of monitored particles (n_o) and monitored area (A_o).

$$n_s = \frac{n_0}{A_0} \tag{2}$$

Calculation of the number of particles per unit volume was performed using a formula from the Ashby and Ebeling [1], which deals with the determination of number, size and spacing of secondary phase particles in extraction replicas.

$$\frac{n_v}{n_s} = \frac{1}{d_{ekv}}\left\{1+\left(\frac{\sigma}{d_{ekv}}\right)^2\right\} \tag{3}$$

where: n_v, number of particles per unit volume; n_s, number of particles per unit area; d_{ekv} , equivalent spherical particle diameter (arithmetic mean); σ , standard deviation of equivalent diameter

The d_{ekv} value was determined from a measured particle area (A_x), according to the following formula:

$$d_{ekv} = \sqrt{\frac{4 \cdot A_x}{\pi}} \tag{4}$$

Particle spacing was determined according to the plane square particle arrangement model, which is suitable for assessing dispersion hardening of low-alloy steel [2]. The calculation was performed in two alternatives as per paper [3]. According to Kelly and Nicolson [4] the mean distance of particle edges is determined from:

$$\lambda = \left(n_v \cdot d_{ekv}\right)^{-1/2} - \sqrt{\frac{2}{3}} \cdot d_{ekv} \tag{5}$$

According to Ashby [5] equation (5) is rectified, due to mutual interaction of dislocation sections after overcoming a particle, as follows:

$$\lambda = 0{,}69 \cdot \left(n_v \cdot d_{ekv}\right)^{-1/2} - \sqrt{\frac{2}{3}} \cdot d_{ekv} \qquad (6)$$

where: d_{ekv}, equivalent particle diameter; λ, mean particle spacing; n_v, number of particles per unit volume. Results are summarised in Table 4.

Table 4. Results of image analysis

sample No.	A_X[nm²]	d_{ekv} [nm]	n_s [m^{-2}]	n_v [m^{-3}]	λ [nm] (Kelly)	λ [nm] (Ashby)
1.0.	168,24	13,65	2,13037.10^{14}	1,79595.10^{22}	52,72	32,92
1.1.	124,01	12,10	7,96117.10^{14}	7,08676.10^{22}	24,26	13,68
1.20.	246,10	16,91	2,81644.10^{14}	1,82597.10^{22}	43,10	25,46

4. FINAL RESULTS AND CONCLUSIONS

Sample 1.1, with the greatest hardness during heat exposure (see Fig. 2), represents an area of additional precipitation of MX particles. This is indicated by the highest number of particles per unit volume, smallest size and smallest mean spacing of particles in comparison to the other samples. In comparison to the initial condition (sample 1.0), the number of particles increased almost fourfold and the mean particle spacing dropped by approx. 2,5 times. In comparison, sample 1.20 most probably represents an area of secondary phase particle coarsening. This is attested to by the greatest mean particle area, significant decrease in number of particles (approx. 4x) and almost a doubled increase in mean particle spacing, when compared to sample 1.1.

The hypothesis that changes occur in the dispersion of the minority phase of weld metal of 14MoV6-3 steel during long-term heat exposure in the sub-creep range has been confirmed. The dominant processes are additional precipitation and coarsening of MX particles. The significant influence of the secondary phase on mechanical properties of 14MoV6-3 steel and matching weld metal is also confirmed by the fact that the dislocation density remained almost unchanged during long-term heat exposure.

Process of additional precipitation causes secondary hardening of CrMoV welds. This fact can lead to embrittlement and also to cracking of welded joint, especially when the temperature of pressure component noticeably decreases. For reduction of this risk it is necessary to carry out proper post weld heat treatment (PWHT). Temperature of PWHT should be higher tan 680°C, optimal temperature range is 720-730°C.

ACKNOWLEDGEMENTS

This result of project LN00B029 was supplied with subvention, resp. supported, by The Ministry of Education of Czech Republic.

REFERENCES

[1] ASHBY, M.F., EBELING, R. On the Determination of the Number, Size, Spacing and Volume Fraction of Spherical Second-Phase Particles from Extraction Replicas, *Transactions of the Metallurgical Society of AIME*, vol. 236, 1966
[2] PRNKA, T. *Doktorská disertační práce*, VŠB Ostrava, VÚHŽ Dobrá, December 1975
[3] PURMENSKÝ, J. Strukturní stabilita nízkolegovaných CrMoV žárupevných ocelí, *kandidátská disertační práce*, VŠB Ostrava, 1978
[4] KELLY, A., NICHOLSON, R.B. Precipitation hardening, *Progress in Material Science*, Vol.10, Chalmers Pergamon Press 1963
[5] ASHBY, M.F. Physics of Strength and Plasticity, *A.S. Argon, MIT Press*, 1969, pg. 113
[6] KOUKAL, J. Teplotní cykly v TOZ svarových spojů nízkolegovaných žárupevných ocelí 15 128 a 15 423, *kandidátská disertační práce*, VŠB, 1975
[7] PURMENSKÝ, J., FOLDYNA, V. Strukturní stabilita nízkolegované CrMoV žárupevné oceli, *Hutnické listy,* 1974
[8] BENEŠ, L.: Mikrostrukturní změny a tvorba „White Etching Layers“ na povrchu provozovaných železničních kolejnic. In: SCIENTIFIC PAPERS OF THE UNIVERSITY OF PARDUBICE, Series B, The Jan Perner Transport Faculty, 9 (2003), str.5-26. ISBN 80-7194-605-2, ISSN 1211-6610